

Optimization of optical beam steering in nonlinear Kerr media by spatial phase modulation

X. D. Cao and D. D. Meyerhofer

Department of Mechanical Engineering, University of Rochester, Rochester, New York 14627, and Laboratory for Laser Energetics, University of Rochester, 250 East River Road, Rochester, New York 14623-1299

G. P. Agrawal

The Institute of Optics, University of Rochester, Rochester, New York 14627

Received December 16, 1993; revised manuscript received June 6, 1994

The optimum conditions for optical beam steering by spatial phase modulation in nonlinear Kerr media are obtained by use of the conservation laws of the nonlinear Schrödinger equation together with the moment method. The operating conditions under which the deflection angle is largest and the deflected beam carries the most energy in the form of a spatial soliton are determined. The analytical theory is applied to both planar waveguides and bulk Kerr media. The analytical predictions are compared with numerical simulations for the case of sinusoidal spatial phase modulation. Good agreement has been found between the analytical results and computer simulations.

1. INTRODUCTION

In general there are three methods for optical beam steering: mechanical, electrical, and all optical. Owing to various problems associated with the mechanical methods, such as difficulties in speed, resolution, and complex fabrication, considerable attention has been paid to electrical and, especially, optical methods. It has been predicted that electrical methods are likely to be limited to operation below 35 GHz because of fundamental considerations such as transit, relaxation, and diffusion times associated with the very-large-scale integrated (VLSI) electronics.¹ For steering devices required for operation at high speeds, optical steering methods play a crucial role, since many nonlinear optical interactions rely on virtual transitions in the material, resulting in an almost instantaneous nonlinear response. Among the variety of nonlinear mechanisms that can be used in optical beam steering, the Kerr effect is invoked most often.²⁻⁵ There are several advantages to using a Kerr medium for optical beam steering. First, the response time of the Kerr nonlinearity can be fast enough that it can be used at switching speeds in excess of 1 THz. Second, it is well known that the propagation of a laser beam in a Kerr medium can be described by the nonlinear Schrödinger equation (NLSE), which supports spatial solitons in the one-dimensional case such as occurs in planar waveguides.⁶ Such spatial solitons can propagate over long distances without spreading, since the nonlinear Kerr effect can compensate for the diffraction-induced beam spreading.

Several optical steering methods based on Kerr media have been proposed.²⁻⁶ Li *et al.*² used an intense pump pulse with a triangular spatial profile to generate a temporal prism inside a nonlinear medium; the temporal prism then deflected another beam passing it.² Another two-beam technique uses cross-phase modulation from a

pump beam to alter the phase profile of a probe beam and so induces a deflection.³ Other authors have employed single beams with asymmetric intensity profiles, resulting in self-bending on propagation.⁴ Another technique uses the properties of dark solitons for beam steering.⁵ Recently Ryan and Agrawal⁶ proposed a new technique that employs spatial phase modulation of a beam entering a nonlinear media, and they showed that high-efficiency beam steering is possible. In their method spatial phase modulation splits the input beam into many subbeams while the nonlinear medium shapes a particular subbeam into a spatial soliton in such a way that most of the power appears in a narrow beam whose direction can be controlled by changes in the modulation parameters.

This paper is devoted to a detailed investigation of optical beam steering by means of spatial phase modulation. Although the numerical simulations of Ref. 6 show efficient beam steering for the situation in which the phase is periodically modulated, it is not clear what phase profile will lead to the best steering conditions from a practical standpoint. Furthermore, it is important to know the conditions under which phase modulation becomes so strong that it will destroy or hinder the formation of a spatial soliton. Our main objective in this paper is to study the conditions under which beam deflection is as large as possible without destroying the soliton nature of beam propagation in the nonlinear medium. We study beam steering in both planar waveguides and bulk media by considering diffraction in one and two transverse dimensions, respectively. In contrast to the results of Ref. 6, where computer simulations were used, we focus mainly on obtaining analytical results, as they are quite valuable in a practical system design. Numerical simulations are used to validate the assumptions and the approximations made in obtaining the analytical results. In Section 2 we describe the analytical approach based on the conservation laws associated with the NLSE. The method

is applied to planar waveguides and bulk Kerr media in Sections 3 and 4, respectively. Finally, the results are summarized in Section 5.

2. CONSERVATION LAWS AND THE VIRIAL THEOREM

Our analytical approach is based on the moment method that makes use of conservation laws associated with the NLSE. The symmetries and the conservation laws of the NLSE have been studied by many authors.⁷⁻¹⁰ In this paper only three conservation laws are needed; they are related to the conservation of the wave action M (equivalent to the conservation of photon number), the transverse momentum \mathbf{P} , and the energy H (or the Hamiltonian of the system). These conservation laws are found to be quite useful in the context of beam steering. For example, the conservation of momentum implies that the beam trajectory, defined as the first moment of the transverse coordinate with respect to the beam intensity (analogous to the center of mass of a mechanical system), is a straight line for a phase-modulated beam. If most of the beam energy is confined inside a newly formed soliton, then this linear trajectory is close to that of the new soliton. By using the laws of conservation of wave action and momentum, one can calculate the deflection angle analytically.

It is well known that the propagation of an intense laser beam in a Kerr medium can be described by a NLSE that, in a normalized form, can be written as⁶⁻¹¹

$$i \frac{\partial A}{\partial z} + \frac{1}{2} \left(\frac{\partial^2 A}{\partial x^2} + \frac{\partial^2 A}{\partial y^2} \right) + |A|^2 A = 0, \quad (1)$$

where x and y are spatial transverse coordinates normalized to the beam width w_0 , z is the propagation distance normalized to the diffraction length, $L_d = kw_0^2$, and the amplitude A is normalized to $(kw_0)^{-1}(n_0/n_2)^{1/2}$. Here $k = 2\pi n_0/\lambda$ is the wave number, λ is the wavelength in vacuum, n_0 is the refractive index of the medium, and n_2 is the Kerr coefficient responsible for self-focusing of the beam. The Lagrangian density corresponding to the NLSE is¹²

$$L = \frac{i}{2} \left(A^* \frac{\partial A}{\partial z} - A \frac{\partial A^*}{\partial z} \right) - \frac{1}{2} \left(\left| \frac{\partial A}{\partial x} \right|^2 + \left| \frac{\partial A}{\partial y} \right|^2 + |A|^4 \right). \quad (2)$$

The application of the Euler-Lagrange equation to the Lagrangian density generates the NLSE given by Eq. (1).

The three conservation laws associated with the NLSE and corresponding to the conservation of the wave action M , the transverse momentum \mathbf{P} , and the energy H (or the Hamiltonian) can be obtained either from Noether's theorem⁷⁻¹⁰ or directly from Eq. (1). These laws are

$$M = \int |A|^2 d^D r, \quad (3)$$

$$\mathbf{P} = \frac{1}{2i} \int (A^* \nabla_T A - A \nabla_T A^*) d^D r, \quad (4)$$

$$H = \frac{1}{2} \int (|\nabla_T A|^2 - |A|^4) d^D r, \quad (5)$$

where we use a compact notation so that Eqs. (3)–(5) can be applied to an arbitrary number of transverse dimensions. In particular, we can apply Eqs. (3)–(5) to one and two transverse dimensions by setting the dimension parameter $D = 1$ and $D = 2$, respectively. The gradient operator ∇_T is defined in D dimensions with respect to the radial vector \mathbf{r} . In one dimension $|\mathbf{r}| = x$, whereas in two dimensions $|\mathbf{r}| = (x^2 + y^2)^{1/2}$. The integration in Eqs. (3)–(5) extends over the entire range of transverse coordinates. The physical meaning of Eqs. (3)–(5) is that the intensity-averaged quantities M , \mathbf{P} , and H remain constant (independent of z) even though the amplitude A changes with z inside the nonlinear medium. In the mechanical analogy M , \mathbf{P} , and H stand for the mass, the momentum, and the energy of a particle.

In the moment method⁷ the average value of a physical quantity $F(\mathbf{r})$ is defined as

$$\langle F(\mathbf{r}) \rangle = \frac{\int F(\mathbf{r}) |A|^2 d^D r}{\int |A|^2 d^D r}. \quad (6)$$

From the standpoint of beam steering the first two moments $\langle \mathbf{r} \rangle$ and $\langle r^2 \rangle$ are of most interest. As mentioned above, the first moment $\langle \mathbf{r} \rangle$ is analogous to the displacement of the center of mass of a mechanical system and indicates the location of the transverse region in which most of the beam energy is likely to be confined in an average sense. The second moment $\langle r^2 \rangle$ can be used to calculate the root-mean-square (rms) beam width s , which is a measure of the size of the area to which most of the beam energy is confined. The rms width s is defined as

$$\sigma^2 = \langle r^2 \rangle - \langle \mathbf{r} \rangle^2. \quad (7)$$

The derivatives $d\langle \mathbf{r} \rangle/dz$ and ds/dz can be used to yield many qualitative features of beam steering in nonlinear media without requiring an explicit solution of the NLSE. The reason is that $d\langle \mathbf{r} \rangle/dz$ is a measure of how much and in what direction the input beam is deflected from the original beam center, and ds/dz indicates how the beam size changes with propagation. By using Eqs. (3)–(6) it is easy to show that $d\langle \mathbf{r} \rangle/dz = \mathbf{P}/M$, i.e., that the conserved momentum determines the beam direction. That the center of mass moves along a straight line as a consequence of momentum conservation has also been noted in Ref. 4. It is not possible to express $d\sigma/dz$ in terms of the conserved quantities. However, the second derivative of σ can be related to M , \mathbf{P} , and H by a standard procedure,¹² a relation also known as the virial theorem.⁷⁻¹⁰ The final result is

$$\frac{d^2 \sigma}{dz^2} = \frac{2}{M} \left(2H + R - \frac{P^2}{M} \right), \quad (8)$$

where R is given by

$$R = \int (1 - D/2) |A|^4 d^D r. \quad (9)$$

It is interesting to note that $R = 0$ only when $D = 2$. For other values of D , R does not vanish. Since R is not a conserved quantity, the exact solution of Eq. (8) can be obtained only when $D = 2$. In the next two sections we

discuss one-dimensional (1D) and two-dimensional (2D) cases separately. The 1D case is applicable mainly to planar waveguides, while the 2D case is applicable to any bulk Kerr medium.

3. BEAM STEERING IN PLANAR WAVEGUIDES

In planar waveguides the optical beam diffracts in only one transverse direction (denoted x) since it is confined in the y direction through the higher refractive index of the waveguide layer compared with that of the cladding layers. The input beam profile is assumed to be Gaussian with a spatially modulated phase $\phi(x)$, so that

$$A(z=0, x) = N \exp(-x^2/2) \exp[i\phi(x)], \quad (10)$$

where the initial peak amplitude N is the usual soliton order^{6,13} and is related to the peak intensity I_0 as $N = kw_0(n_2 I_0/n_0)^{1/2}$ in the normalized units used here. The use of Eq. (10) in Eqs. (3)–(5) with $D = 1$ allows us to calculate the three conserved quantities M , P , and H . These constants can then be used to calculate the variation of the first two moments $\langle x \rangle$ and $\langle x^2 \rangle$.

A. Beam Deflection and Soliton Condition

The extent of beam deflection is quantified by $\langle x \rangle$, a quantity that represents the deviation of the beam from the center of the input beam located at $x = 0$. As was discussed in Section 2, $\langle x \rangle$ evolves with z as

$$\frac{d}{dz} \langle x \rangle = \frac{P}{M}, \quad (11)$$

where the momentum is denoted as a scalar quantity because it is always directed toward the x axis in the 1D case. Since both P and M are conserved, the trajectory of $\langle x \rangle$ from the original beam center (located at $x = 0$) is a straight line making a deflection angle $\theta_{\text{def}} = P/M$ with respect to the z axis. Equations (4) and (10) give

$$\theta_{\text{def}} = \frac{P}{M} = \frac{1}{\sqrt{\pi}} \int \frac{d\phi}{dx} \exp(-x^2) dx. \quad (12)$$

Equation (12) predicts how the beam center of an input Gaussian beam is deflected as a result of spatial modulation of the phase. A similar result can be obtained for other intensity profiles. Since our analysis relies on the conserved quantities (M , P , and H), which are obtained by integrating over the beam profile [Eqs. (3)–(5)], the exact beam shape is not important, and the results obtained for a Gaussian beam apply qualitatively for other beam profiles as well.

Practical applications of beam steering require that phase modulation causes the beam to change only its direction of propagation (or at least causes most of the beam power to be switched to that direction) without a change in the beam width and the beam power. The beam width will not increase substantially only if the input beam propagates as a spatial soliton after the phase modulation. By using Eq. (8), we can find the condition under which the spatial soliton can tolerate the perturbation. If the right side of Eq. (8) is less than or equal to zero, the rms beam width s can only decrease with propagation.

It has been shown that the Hamiltonian H is bounded in such a way^{14,15} that the right-hand side of Eq. (8) cannot be negative in the 1D case because the beam width does not decrease to zero (there is no catastrophic self-focusing). Hence the condition for forming a spatial soliton is determined when we set the right-hand side of Eq. (8) equal to zero. The same argument was used to find the threshold value of soliton amplitude in birefringent optical fibers, with good agreement between the analytical results and numerical simulations.¹⁶ Since H , M , and P are constants, there is only one unknown quantity, R , on the right-hand side of Eq. (8). Following the method used in Ref. 16, we can estimate R by using the Schwartz inequality under the assumption that the beam energy is confined within a spatial region of a finite width W . The result is given by

$$R > \frac{1}{2} \frac{M^2}{W}. \quad (13)$$

By using inequality (13) in Eq. (8), we can write the soliton condition $d^2\sigma^2/dz^2 = 0$ as

$$N^2 > \frac{1}{(\sqrt{2} - \sqrt{\pi}/W)} \times \left[1 - 2(\theta_{\text{def}})^2 + \frac{2}{\sqrt{\pi}} \int \left(\frac{d\phi}{dx} \right)^2 \exp(-x^2) dx \right]. \quad (14)$$

Equation (12) and inequality (14) constitute the main analytical results of this section. They can be applied to arbitrary phase profiles $f(x)$. Before considering the specific case of sinusoidal phase modulation, we consider a linear phase tilt that is equivalent to placing a prism in the beam path. The phase profile $f(x)$ then takes the following simple form:

$$\phi(x) = 2\pi px, \quad (15)$$

where p is a constant related to the amount of phase tilt. The deflection is obtained from Eq. (12) and is given by

$$\theta_{\text{def}} = 2\pi p. \quad (16)$$

It is straightforward to show that a linear phase tilt has no effect on soliton propagation except a change in the propagation direction of the soliton. In fact, Li *et al.*² used an intense pump beam to generate a temporal prism and to bend another beam. Although it is conceptually simple to use a linear phase tilt, it may not be easy to implement one in practice.

B. Analytical Results for Sinusoidal Phase Modulation

The interesting case from the standpoint of beam steering is that of periodic phase modulation, because such a modulation can be easily applied in practice by use of a phase grating.⁶ At the same time sinusoidal modulation permits closed-form evaluation of the integrals appearing in Eq. (12) and inequality (14), resulting in simple expressions for the steering angle and the soliton condition. The functional form of the phase is given by

$$\phi(x) = \phi_0 \sin(2\pi px + \delta), \quad (17)$$

where ϕ_0 is the amplitude of the modulation, p is the spatial modulation frequency, and δ is a constant phase

shift. By substituting Eq. (17) into Eq. (10) and using a standard Bessel-function expansion of the phase term $\exp[i\phi(x)]$, one can see that the phase modulation breaks an input beam into multiple subbeams propagating at different angles¹⁷ (Raman-Nath scattering):

$$A(z=0, x) = N \exp(-x^2/2) \sum_{m=-\infty}^{\infty} J_m(\phi_0) \times \exp[im(2\pi p x + \delta)]. \quad (18)$$

The initial amplitude of various subbeams is determined through the modulation amplitude ϕ_0 , while the steering angles are determined by the modulation frequency p in the linear regime. To understand the nonlinear propagation of multiple interacting beams in a Kerr medium, it is useful to look at its analogy in the time domain provided, for example, by the propagation of solitons in birefringent optical fibers.¹⁶ Just as the Kerr nonlinearity can negate the modal dispersion between the fast and the slow modes and fuse two subpulses propagating along the fast and the slow axes of a birefringent fiber to form a single solitary wave (so-called soliton trapping), the same nonlinearity can also negate the spatial dispersion (or diffraction) between several subbeams. The physical meaning of this analogy is that it is possible to divert power from various subbeams and form a single spatial soliton. From the case of linear phase tilt, it is easy to see that each subbeam propagates at an angle equal to $2\pi m p$.

We now proceed to calculate the deflection angle of the beam center. By using Eqs. (12) and (17), we obtain a simple analytical result

$$\theta_{\text{def}} = 2\pi p \phi_0 \cos \delta \exp(-\pi^2 p^2). \quad (19)$$

An important conclusion from Eq. (19) is that the deflection angle is largest for an optimum value p_{opt} of the spatial modulation frequency. This feature is quite understandable physically. If the modulation frequency is too high, it will tend to destroy the soliton. On the other hand, beam deflection will be small for small modulation frequencies, since the phase variation across the beam is then relatively flat. This optimum value of p is obtained by maximizing θ_{def} and is given by $p_{\text{opt}} = \sqrt{2}/2\pi = 0.225$. It should be noted that optimal value of p is a consequence of sinusoidal phase modulation that requires a trade-off between two conditions: (1) the maximum of the phase slope is at the center of the incident beam, which demands high values of the spatial frequency, and (ii) the sinusoidal function is still close to the linear function within the beam size, which demands low values of the spatial frequency p .

The soliton condition is obtained by using relation (14) and becomes

$$N^2 > \frac{1}{\sqrt{2}} \{1 + 4\pi^2 p^2 \phi_0^2 [1 + \cos(2\delta) \exp(-4\pi^2 p^2)] - 2 \cos^2 \delta \exp(-2\pi^2 p^2)\}, \quad (20)$$

where $W \gg 1$ was assumed. This condition states that the deflected beam can form a spatial soliton if N exceeds a critical value determined by various modulation parameters. Equation (20) can be simplified for $2\pi p \ll 1$ and becomes

$$N^2 > \frac{1}{\sqrt{2}} [1 + 16\pi^4 p^4 \phi_0^2 (1 - \cos^2 \delta)]. \quad (21)$$

Relations (19) and (21) indicate that it is always best to choose $\delta = 0$ or π , since such values of δ increase the deflection angle and decrease the input power required for forming a spatial soliton. This is understandable physically, since $\delta = 0$ or $\delta = \pi$ means that the beam center experiences a linear phase tilt when p is small. As was mentioned above, a linear phase tilt causes the beam to change direction without affecting the soliton mode of propagation. Equation (19) and inequality (21) also suggest that the larger modulation depths ϕ_0 are better for beam steering. However, this is not the case, as is explained in Ref. 6. As is seen from Eq. (18), the amount of power initially present in a subbeam depends critically on the modulation amplitude ϕ_0 through the factor $J_m(\phi_0)$. The ideal choice of modulation amplitude is therefore $\phi_0 = 2.405$, the first zero of J_0 , since in that case phase modulation leaves no power in the central, undeflected portion of the beam. For $\delta = 0$ (or π) and $p_{\text{opt}} = \sqrt{2}/2\pi = 0.225$, inequality (20) reduces to $N^2 > (1 + 0.8\phi_0^2)/\sqrt{2}$. By using $\phi_0 = 2.405$, one finds that a spatial soliton with maximum deflection can be formed when N exceeds 2.

C. Numerical Simulations

To verify the extent to which the analytical results are applicable in practice, we solve Eq. (1) numerically with the well-known split-step method.¹³ Figure 1 shows the propagation of an input Gaussian beam for six values of the spatial frequencies in the range p equal to 0.1–0.3 by choosing $\phi_0 = 2.405$, $\delta = 0$, and $N = 1$ in Eq. (10). The straight lines in Figs. 1(a)–1(f) show the trajectory of the beam center $\langle x \rangle$ as predicted by Eq. (11). As predicted by Eq. (19), the deflection angle is largest when $p = \sqrt{2}/2\pi = 0.225$, as shown in Fig. 1(c). The results of the numerical simulation agree quite well with the analytical predictions. When the spatial frequency is small ($p < 0.2$), the phase perturbation does not affect the formation of the spatial soliton other than changing its direction of propagation as shown in Figs. 1(a) and 1(b). The absence of other subbeams indicates that energy from these subbeams has been channeled into the main subbeam as a result of the spatial analog of soliton trapping. When p becomes larger than 0.2, a small amount of energy begins to show up in the subbeams, which means that the main subbeam intensity is not large enough to hold all the subbeams together, as the case in Figs. 1(a) and 1(b). At the same time the main beam is no longer a spatial soliton, since the beam width increases as the beam propagates along the Kerr medium. This broadening can be seen from Figs. 1(c)–1(f).

The validity of Eq. (19) for the deflection angle over a wide range of values of the parameter p is evident in Fig. 2, where the predicted dependence of θ_{def} on the modulation frequency p is compared with numerical simulations. The predicted values of θ_{def} are plotted as a continuous curve, while the results of computer simulations are plotted as squares. The theory agrees exactly with the computer simulations. To make the main subbeam propagate as a spatial soliton for $p > 0.2$, more power is needed. The extra power needed to compensate for

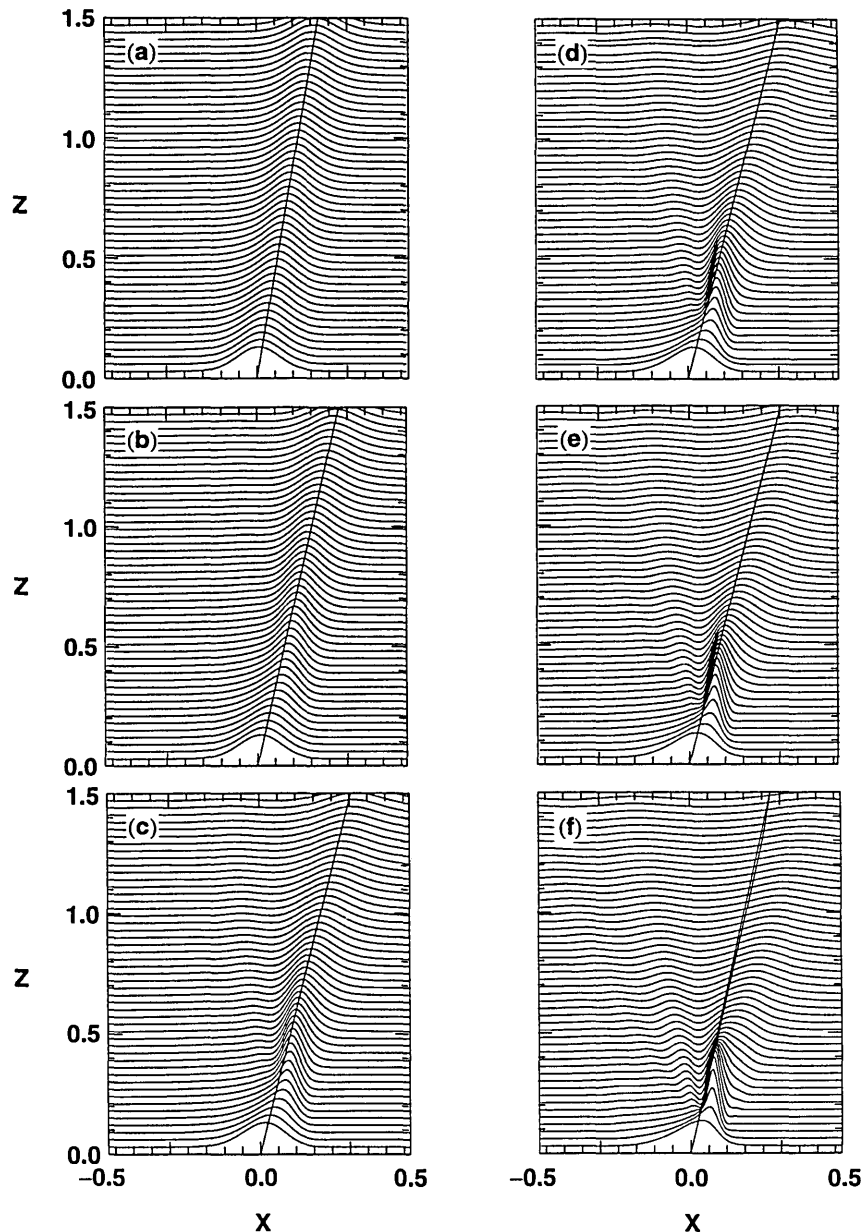


Fig. 1. Propagation of beam intensity for various spatial modulation frequencies. (a) $p = 0.1$, (b) $p = 0.15$, (c) $p = 0.20$, (d) $p = p_{\text{opt}} = 0.225$, (e) $p = 0.25$, (f) $p = 0.30$. The other parameters are $\phi_0 = 2.405$, $\delta = 0$, and $N = 1$.

the phase modulation can be calculated from inequality (20). For example, for a spatial soliton to be formed when $p = 0.225$, the initial amplitude N should be increased from 1 to 1.63. Figures 3(a) and 3(b) compare the beam propagation when $N = 1$ and $N = 1.63$. Clearly the deflected beam propagates as a fundamental soliton when the input peak amplitude is increased from 1 to 1.63. Therefore Eq. (19) and inequality (20) are quite accurate in predicting the optimal choice of input beam parameters when spatial phase modulation is used for beam steering.

4. BULK KERR MEDIA

An important difference between 1D and 2D beam steering is that the optical beam can collapse catastrophically in 2D, a feature that is well known in the theory of self-focusing.⁷⁻¹⁰ However, catastrophic self-focusing

or beam collapse can be easily avoided in practice by the choice of a medium length shorter than the critical self-focusing distance. Thus with proper choice of the medium length the beam-steering technique would work well even in a bulk Kerr medium. Although there are no stable soliton solutions of the NLSE in the 2D case, the self-trapping condition is analogous to the 1D case. Mathematically, the 2D problem is easier to solve than the 1D case, since the unknown term R in Eq. (8) is exactly zero, as can be seen by setting $D = 2$ in Eq. (9). Therefore Eq. (8) can be solved exactly. As an illustration, consider the case of periodic phase modulation in both transverse coordinates. The spatially modulated input amplitude is then given by

$$A(z=0, x, y) = N \exp[-(x^2 + y^2)/2] \times \exp[i\phi_1 \sin(2\pi p_1 x + \delta_1) + i\phi_2 \sin(2\pi p_2 y + \delta_2)], \quad (22)$$

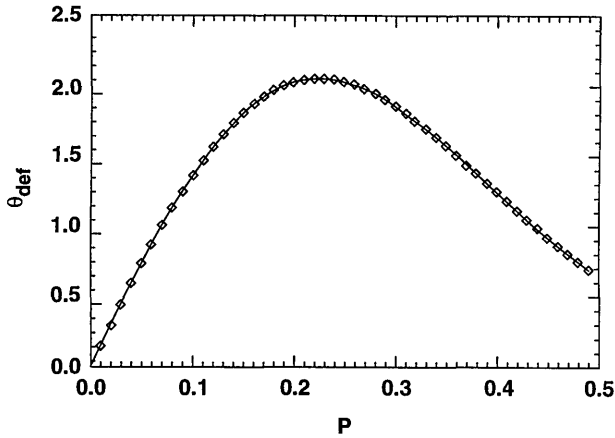
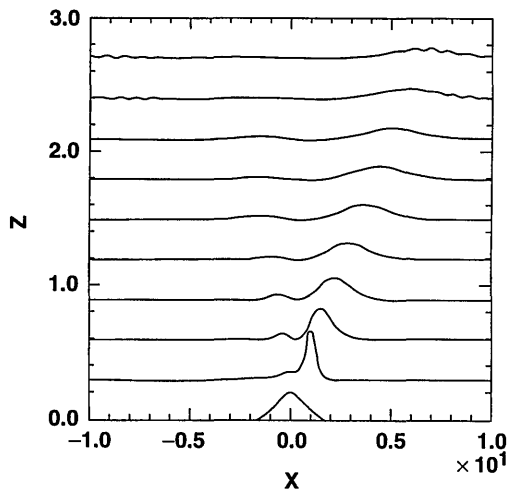
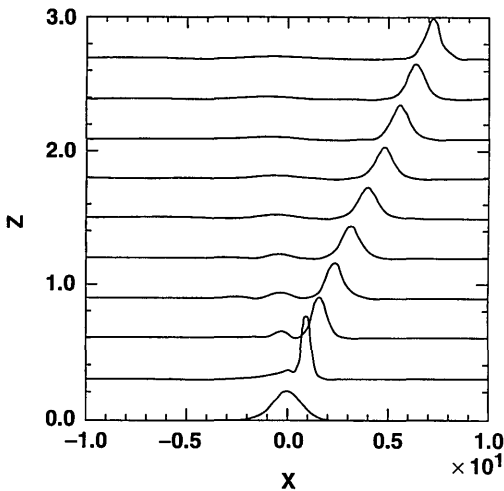


Fig. 2. Dependence of deflection angle on modulation frequency p . The solid curve and the data points (squares) are obtained from the analytical theory and the computer simulations, respectively.



(a)



(b)

Fig. 3. Effect of input power on beam steering. (a) $N = 1$; the soliton is destroyed by spatial phase modulation. (b) $N = 1.61$; the deflected beam propagates as a fundamental spatial soliton.

where p_1 and p_2 are spatial frequencies in the two transverse directions. By following a procedure similar to that used in the 1D case, we find that the deflection angles in the two directions are given by

$$\theta_i = 2\pi p_i \cos(\delta_i) \exp(-\pi^2 p_i^2), \quad i = x, y. \quad (23)$$

From Eq. (23) the optimum modulation frequency for maximum beam deflection in either transverse direction is just $p_i = \sqrt{2}/2\pi = 0.225$. This decoupling of the x and the y directions is due to the specific form of the input field. As is seen from Eq. (22), the input field itself is separable in x and y . The condition for self-trapping of the optical beam is similar to inequality (20) and can be written as

$$N^2 = 2 + \sum_{i=1}^2 (2\pi p_i)^2 [1 + \cos(2\delta_i) \exp(-4\pi^2 p_i^2) - 2 \cos^2 \delta_i \exp(-2\pi^2 p_i^2)], \quad (24)$$

where we used the fact that $M = \pi N^2$. It is well known that $M = 2\pi$ is the critical-power self-trapping of an unmodulated beam in the 2D case.⁷⁻⁹ Equation (8) reduces to $N^2 = 2$ and $M = 2\pi$ when p_1 and p_2 are set to zero. It is important to note that Eq. (24) represents an exact solution of Eq. (8) that we obtained by setting the right-hand side of Eq. (24) equal to zero (for the case of self-trapping). This is quite different from the condition [inequality (20)] that provides only an approximate lower bound. The difference is due to the vanishing of the quantity R , defined by Eq. (9), in the 2D case. In practice the power required for self-trapping need not be exact as given by Eq. (24); in other words, it can be larger than the value given by

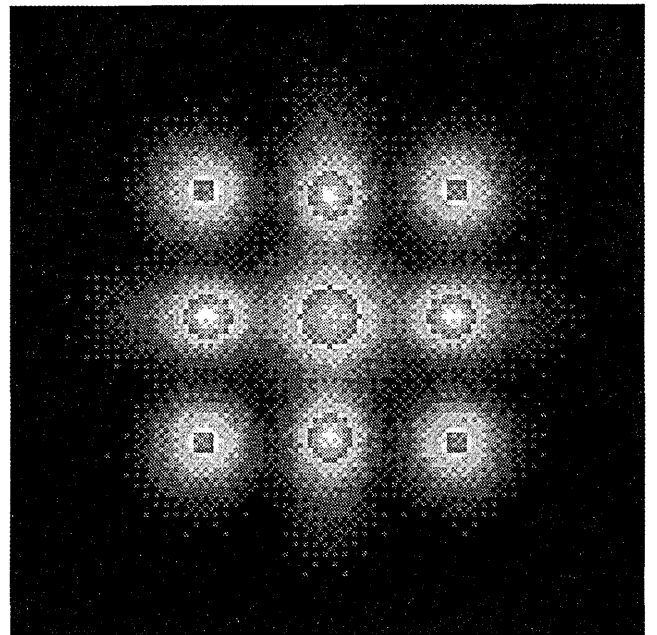


Fig. 4. Simulated contour plots of beam intensity at a distance $z = 1.5$ in bulk Kerr media for nine different values of the modulation parameters. The center spot corresponds to the undeflected output beam in the absence of any phase modulation. The four spots at the corners are the deflected beams when $p_1 = p_2 = 0.225$ and δ_1 and δ_2 are set to 0 or π . The other four spots along the sides are the deflected beams when the phase is modulated along only one transverse dimension. The other parameters are $\phi_1 = \phi_2 = 2.405$ and $N = \sqrt{2}$.

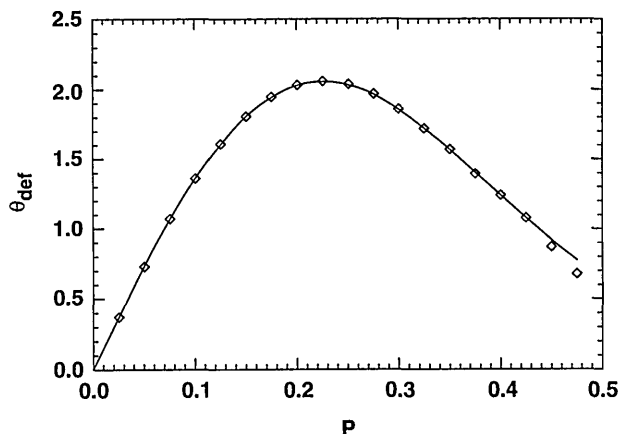


Fig. 5. Dependence of deflection angle on modulation frequency p in bulk media. The solid curve and the data points (squares) are obtained from the analytical theory and the computer simulations, respectively.

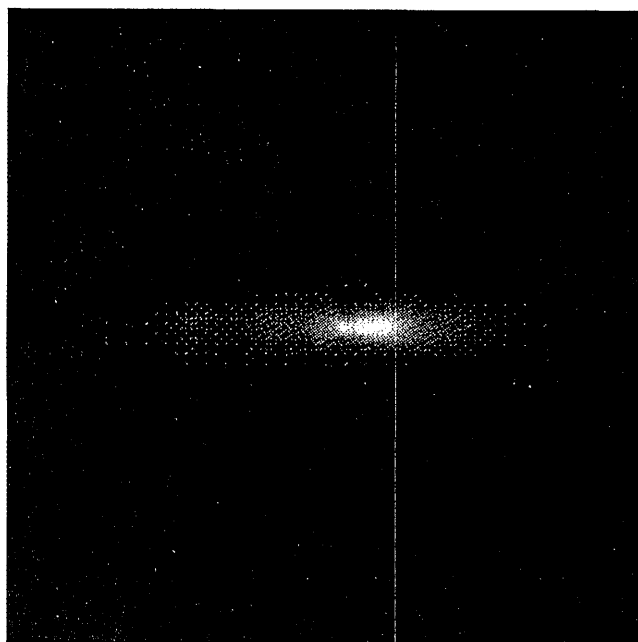


Fig. 6. Deflected beam when the modulation frequency p_1 is changed from 0.025 to 0.5. The other parameters are $p_2 = 0$, $\phi_2 = 0$, $\phi_1 = 2.405$, $\delta_1 = 0$, and $\delta_2 = 0$.

Eq. (24) as long as the medium is much shorter than the self-focusing distance.

To study the usefulness of beam steering in bulk Kerr media, we have performed a numerical simulation using a computational grid of size 128×128 to represent the input Gaussian beam in the two transverse dimensions. The calculations were performed on a Cray supercomputer because of the three-dimensional nature of the problem. Figure 4 shows the intensity contour plots for nine choices of the modulation parameters obtained with $\phi_1 = \phi_2 = 2.405$ and $N = \sqrt{2}$ (corresponding to $M = 2\pi$). The nine cases correspond to various combinations of the phases (δ_1 and δ_2) and spatial frequencies (p_1 and p_2). In particular, $\delta_1 = 0$ or $\delta_1 = p$, depending on whether the beam deflects to the right or the left; $\delta_2 = 0$ or $\delta_2 = p$, depending on whether the beam deflects upward or downward; and p_1 and p_2 take values of 0 or 0.225 (the

optimum value), depending on whether the phase is modulated along x , y , or both axes.

To see the beam deflection in the transverse plane (xy plane), we plot the input beam spot (the center one) and the deflected beam spots in Fig. 4. All the deflected beams start from the same input position (the center in Fig. 4). Note that the deflected beams are overplotted in Fig. 4; in fact they are the results of eight individual simulations, corresponding to eight different spatial modulations. The four spots at the corners are the deflected beams when $p_1 = p_2 = 0.225$. One can control their positions by changing the value of δ_1 or δ_2 . The other four spots along the sides are the deflected beams when phase is modulated along only one transverse dimension. The propagation distance is the same as that of Fig. 1 ($z = 1.5$). The four central spots along the side lines are brighter than the four at the corners because the perturbation is weaker when phase is modulated along only one transverse direction. The main subbeam carries less energy if the perturbation is stronger, since more energy is diverted to other subbeams. The spot sizes of the deflected beams are in fact smaller than that of the input beam. This is not caused by self-focusing, since the self-focusing distance is much longer than 1.5. The focusing effect is caused by phase modulation and is similar to that seen in Fig. 1 in the 1D case. After some energy is diverted into multiple subbeams, the main subbeam is compressed to conserve the total momentum.

To test the accuracy of Eq. (23), we plot the deflection angle obtained numerically as a function of the modulation frequency p_1 in Fig. 5. It is obvious that an optimum frequency exists and is ~ 0.225 , as predicted analytically. Similar to the 1D case shown in Fig. 2, Fig. 5 also shows excellent agreement between the theoretical predictions and computer simulations. Figure 6 shows how the beam is deflected when the modulation frequency p_1 is changed from 0.025 to 0.5. Since the spatial modulation is applied only to the x axis, the beam spots are deflected along the x axis. As the modulation frequency p increases, the beam is reflected further to the right. When p_1 is small, the beam width is almost a constant. When p is larger than 0.2, the beam becomes broadened, and some energy goes to the other direction. When p approaches 0.5, the subbeams become as strong as the main beam.

5. CONCLUSIONS

The technique of optical beam steering by spatial phase modulation and its optimization is discussed with an analytical approach based on the conservation laws associated with the NLSE. We use the moment method to find the first two moments ($\langle x \rangle$ and $\langle x^2 \rangle$ in the 1D case), which govern the deflection of the beam center and the rms beam width, respectively. Even though our theory is valid for an arbitrary form of spatial phase modulation, we have considered mainly the case of sinusoidal phase modulation. It is found that there is an optimal spatial frequency for the sinusoidal phase modulation for which the deflection is largest. In normalized units this optimum value is $p = 0.225$. Since the transverse coordinates in Eq. (1) are scaled with the beam width w_0 , the optimum spatial frequency is $0.225/w_0$ irrespective of

other beam and medium parameters. For instance, the optimum deflection angle $\theta_{\text{def}} = 3.58$ mrad when the laser wavelength $\lambda = 1 \mu\text{m}$ and $w_0 = 10 \mu\text{m}$. In spite of the relative small value of the deflection angle, the steering resolution can be quite high. The reason is that diffractive effects are nearly canceled by the soliton nature of the steered beam. The spatial resolution increases linearly as the increasing length of the nonlinear medium. It is interesting to note that most of the beam power is confined to a single modulation cycle under optimum operating conditions. The moment method also allows us to obtain the input beam power required for steering the beam as a spatial soliton (1D case) or as a self-trapped beam (2D case). Surprisingly, whereas an exact expression can be obtained in the 2D case (bulk Kerr media), only an approximate lower bound is found in the 1D case (planar Kerr waveguides).

To verify the analytical predictions of the moment method, we have performed numerical simulations in both waveguide and bulk Kerr media by considering the 1D and 2D cases separately. Good agreement has been found between the analytical theory and computer simulations in both cases. An advantage of our analytical results is that they are exact in the 2D case. Usually it is computationally expensive to simulate beam propagation in bulk nonlinear media, making it difficult to explore the multidimensional parameter space. Our analytical results should prove useful in the design of optical systems that exploit nonlinear optics for beam steering and make use of a bulk Kerr medium for this purpose.

ACKNOWLEDGMENTS

X. D. Cao thanks W. Wang for useful discussions. The research of G. P. Agrawal is supported by the U.S. Army Research Office. X. D. Cao and D. D. Meyerhofer are

supported by the U.S. Department of Energy, Office of Inertial Confinement Fusion, under Cooperative Agreement DE-FC03-92SF19460, the University of Rochester, and the New York State Energy Research and Development Authority.

REFERENCES

1. P. W. Smith, *Bell Syst. Tech. J.* **61**, 1975 (1982).
2. Y. Li, D. Y. Chen, L. Yang, and R. R. Alfano, *Opt. Lett.* **16**, 438 (1991).
3. A. J. Stentz, M. Kauranen, J. J. Maki, G. P. Agrawal, and R. W. Boyd, *Opt. Lett.* **17**, 19 (1992).
4. G. A. Swartzlander, Jr., H. Yin, and A. E. Kaplan, *Opt. Lett.* **13**, 1011 (1988); *J. Opt. Soc. Am. B* **6**, 1317 (1989); Y. J. Ding, C. L. Guo, G. A. Swartzlander, Jr., J. B. Khurgin, and A. E. Kaplan, *Opt. Lett.* **15**, 1431 (1990).
5. B. Luther-Davies and X. Yang, *Opt. Lett.* **17**, 1755 (1992).
6. A. T. Ryan and G. P. Agrawal, *Opt. Lett.* **18**, 1795 (1993).
7. F. H. Berkshire and J. D. Gibbon, *Stud. Appl. Math.* **69**, 229 (1983).
8. J. J. Rasmussen and K. Rypdal, *Phys. Scr.* **33**, 481 (1986).
9. K. Rypdal and J. J. Rasmussen, *Phys. Scr.* **33**, 498 (1986).
10. V. E. Zakharov, V. V. Sobolev, and V. S. Synakh, *JETP Lett.* **14**, 390 (1971).
11. V. I. Talanov, *JETP Lett.* **2**, 138 (1965).
12. C. J. McKinstrie and D. A. Russell, *Phys. Rev. Lett.* **61**, 2929 (1988).
13. G. P. Agrawal, *Nonlinear Fiber Optics* (Academic, Boston, 1989).
14. V. E. Zakharov, E. A. Kuznetsov, and A. M. Rubenchik, in *Solitons*, S. E. Trullinger, V. E. Zakharov, and V. L. Pokrovsky, eds. (North-Holland, New York, 1986), Chap. 10, p. 503.
15. V. K. Mesentsev and S. K. Turitsyn, *Opt. Lett.* **17**, 1497 (1992).
16. X. D. Cao and C. J. McKinstrie, *J. Opt. Soc. Am. B* **10**, 1202 (1993).
17. A. Yariv and P. Yeh, *Optical Waves in Crystals: Propagation and Control of Laser Radiation* (Wiley, New York, 1984), Chaps. 8–10.